

# Absolute hadron beam polarimetry at EIC

Frank Rathmann

EIC Group Meeting

<https://indico.bnl.gov/event/26587/>

February 20, 2025

# Initial observation

- In recent years, many groups specializing in **polarization instrumentation & technology** for hadronic probes have disappeared, along with the valuable expertise they once contributed. This contrasts sharply with the time when RHIC was conceived, when numerous experimental and theoretical groups from around the world provided a wealth of expertise.
- Currently, we face a critical situation, with a shortage of skilled individuals, which is crucial to overcome for the EIC's success.
- There is an urgent need to rejuvenate polarization instrumentation & technology for hadrons and expand education and training efforts.<sup>1</sup>

---

<sup>1</sup>Key areas are highlighted in <https://technotes.bnl.gov/PDF?publicationId=225693>

# Contents I

- 1 Introduction
  - Polarimetry requirements for the EIC
  - Asymmetry, polarization, instruments
  - Absolute beam polarization
- 2 Beam-induced target depolarization
  - Bunch-induced depolarization at RHIC and EIC
  - Magnetic fields from beam charge at RHIC and EIC
- 3 Magnetic guide field for the polarized jet at EIC
  - Spin-dependent cross section
  - Guide field concept
- 4 Other polarized beams
  - Absolute  $^3\vec{\text{He}}$  and  $\vec{d}$  polarimetry
  - Status of polarimetry section in IP4 at EIC
- 5 Will carbon fiber targets survive at EIC?
  - Direct temperature measurement using light from Carbon targets
- 6 Conclusion and Outlook

# Hadron polarimetry requirements for the EIC I

## Comments

- The EIC will use polarized **protons** and **helions**, later on possibly deuterons, and heavier nuclei like lithium may be needed.
- **The EIC promises to provide proton beam polarizations of  $P \geq 0.7$  with a relative uncertainty of  $\Delta P/P \leq 1\%$ .**
- Polarization calibration needed for each ion species as presently done:
  - elastic scattering of identical particles  $\Rightarrow$  beam polarization inferred from known target polarization.
- **Absolute proton beam polarization calibration relies on precisely measured nuclear polarization of atomic jet using Breit-Rabi polarimeter.**



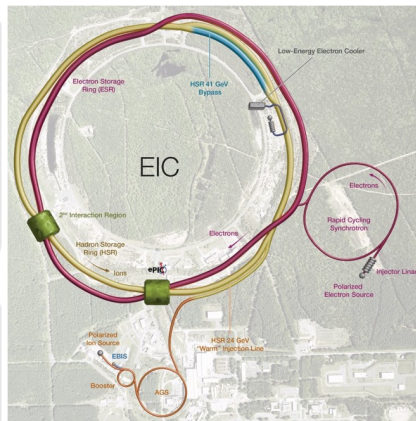
# Hadron polarimetry requirements for the EIC II

## Polarimeters shall determine:

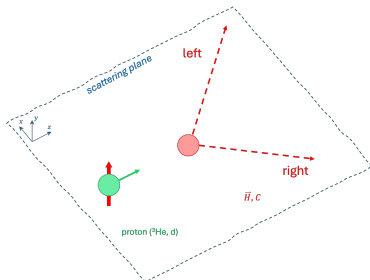
- Bunch polarization profile in  $x$ ,  $y$ ,  $z$
- Polarization lifetime
  - For EIC physics, projection of  $\vec{P}$  on stable spin axis required, no in-plane polarization.
- Polarization vector  $\vec{P}$  per bunch

## Instruments

- Hadron polarimeter (absolute) in IP4
- pC polarimeter (relative) in IP4 and IP6 (between spin rotators)



# Asymmetry and polarization



- Spin-dependent cross section

$$\sigma = \sigma_0(1 + A_y P_y \cos \phi) \quad (1)$$

- Unpolarized cross section  $\sigma_0$
- $P_y$  vertical component of beam polarization  $\vec{P} = (P_x, P_y, P_z)$
- Analyzing power  $A_y = \frac{\sigma^{\text{left}} - \sigma^{\text{right}}}{\sigma^{\text{left}} + \sigma^{\text{right}}}$
- Azimuth of scattered particle  $\phi$

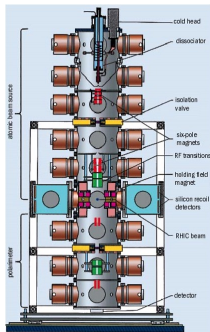
## Coulomb-nuclear interference (CNI) (see slide 65).)

- $A_y$ : measure of polarization sensitivity of scattering process
- **At AGS and RHIC energies, no scattering processes available with  $A_y$  known to sufficient accuracy for  $\Delta P/P \leq 0.01$  [1].**
- **Interference of EM and strong interaction at small scattering angles provides sizable analyzing power for elastic  $pp$  (and  $pN$ ) scattering.**

# Instruments for absolute and relative polarimetry

## Two devices

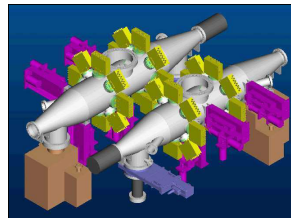
- **HJET polarimeter**



- **absolute, slow**

$$\frac{\Delta P}{P} \approx 3\% \text{ per 4 hour} \quad (2)$$

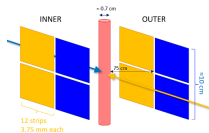
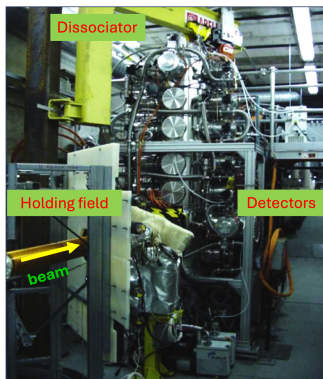
- **pC polarimeters**



- **fast, relative**
- **transverse profiles of polarization**

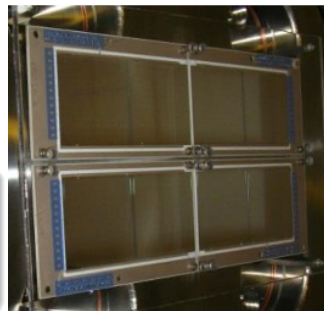
$$\frac{\Delta P}{P} < 1\% \text{ per scan} \quad (3)$$

# Detector system at the polarized jet target



Eight Si strip detect.

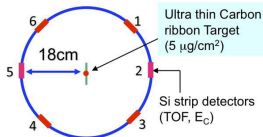
- 12 vertical strips
- 3.75 mm pitch
- 500 μm thickness



With present setup of L-R detectors and guide field  $B_y$

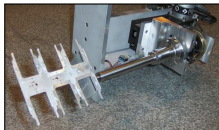
- Only vertical component  $P_y$  measurable via L-R asymmetry near  $\theta = 90^\circ$ .

# CNI polarimeter setup



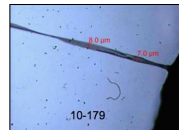
CNI setup with 6 Si detectors at different azimuth at each target enables

- determination of polarization components  $P_x$  and  $P_y$
- determination of polarization profile along  $x$  and  $y$
- Due to parity violation,  $A_z \approx 0$  (no longitudinal analyzing power)  $\rightarrow P_z$  not measurable with *unpolarized* target



## Ultra-thin ribbon targets

- 8 target holder inside beam pipe
- 2 holders per beam for  $x$  and  $y$
- 6 targets per holders, 48 in total
- Targets  $\approx 10 \mu\text{m} \times 100 \text{ nm}$ , hand crafted by D. Steski & team



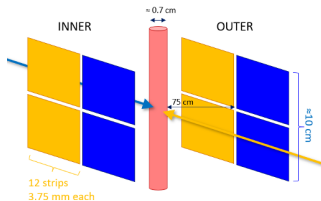
# Absolute polarization from polarized hydrogen jet I

## Breit-Rabi polarimeter

- Capable to determine absolute polarization  $Q$  of atomic beam, i.e., electron and proton polarization of hydrogen atoms, with accuracy  $\Delta Q/Q \lesssim 1\%$ .
  - Take this as a given. Will revisit subject through measurements after run 25.
  - No solid estimates available that fully encapsulate the BRP measurement systematics at the HJET on the  $\approx 1\%$  level.

## Beam polarization calibration

1. Proton beam passes through target of polarized H atoms of known polarization  $Q$



# Absolute polarization from polarized hydrogen jet II

## Beam polarization calibration

2. Measure number of scattered particles in left (L) and right (R) detectors
3. Sign of  $Q$  periodically reversed to compensate for asymmetries caused by differences in detector geometry or efficiency in L and R directions.
4. This determines target asymmetry

$$\epsilon_{\text{target}} = \frac{L - R}{L + R} = A_y \cdot Q \cos \phi. \quad (4)$$

5. Measurement of corresponding asymmetry with beam particles determines  $\epsilon_{\text{beam}}$ . In elastic  $pp$  scattering, and more general in the elastic scattering of *identical* particles,  $A_y$  same regardless of which proton is polarized.
6. Absolute beam polarization given by

$$P = \frac{\epsilon_{\text{beam}}}{\epsilon_{\text{target}}} \cdot Q \quad (5)$$

# Beam-induced target depolarization at RHIC and EIC

## Polarized hydrogen jet

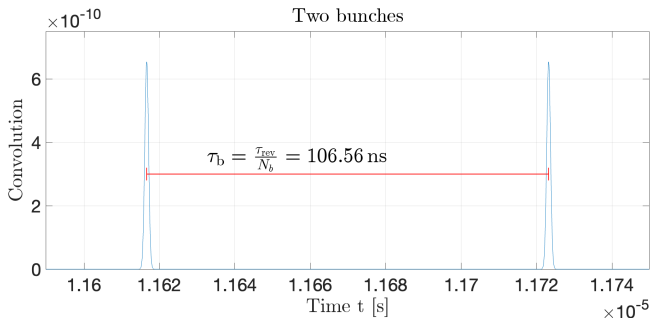
- Development of HJET for RHIC finished  $\approx 20$  yrs ago.
- Many details on the technical structure and development cannot be found in the literature. There is no comprehensive publication available.
- Grigori Atoian knows all that is needed to reliably operate the source
- Anatoli Zelenski is an excellent source of information
  - Tom Wise gave me some unfinished paper drafts and notes.
  - I am in touch with Alexander Nass about BRP operation and his most recent full polarization measurement with BRP (from 2004).
- At EIC, bunch repetition frequency much larger than at RHIC  $\rightarrow$  investigate **beam-induced depolarization of target atoms** and understand situation



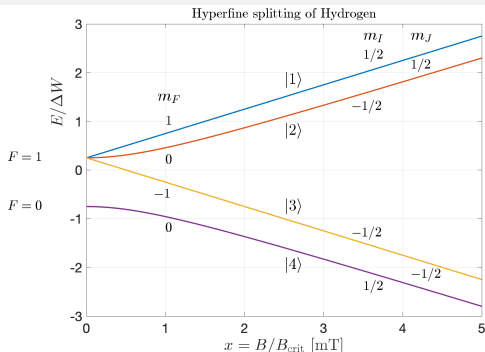
# Bunch structure

## RHIC situation:

- Time period between two adjacent bunches:  $\tau_b = \frac{\tau_{\text{rev}}}{N_b} = 106.57 \text{ ns}$
- Number of stored bunches  $N_b = 120$
- Bunch frequency  $f_b = \frac{1}{\tau_b} = 9.3831 \text{ MHz}$
- Large number of harmonics contribute to induced magnetic high-frequency field close to RHIC beam, as bunches are short ( $\sigma_t \approx 1.8 \text{ ns}$ )



# Hyperfine states of hydrogen



Critical field  $B_c$  (see slide 67)

- Zeeman energy  $g_J \mu_B B$  comparable to  $E_{\text{hfs}}$
- $E_{\text{hfs}} \approx 5.874 \times 10^{-6} \text{ eV}$  ( $\approx 1420 \text{ MHz}$  [2]):
- $B_c = 50.7 \text{ mT}$

## Transition frequencies

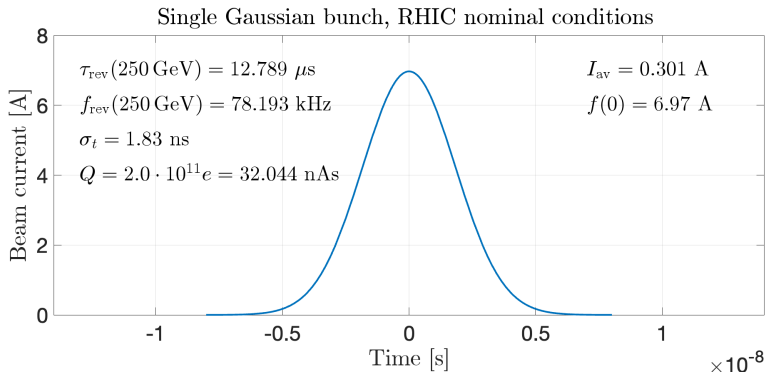
- Transition frequency between two hyperfine states  $|i\rangle$  and  $|j\rangle$  given by:

$$f_{ij} = \frac{E_{|i\rangle}(B) - E_{|j\rangle}(B)}{h} \quad (6)$$

- When  $f_{ij}$  matches one of the beam harmonics at a certain holding field  $|\vec{B}|$ , resonant depolarization occurs [3]

# Single bunch distribution

- (Gaussian) bunch in RHIC



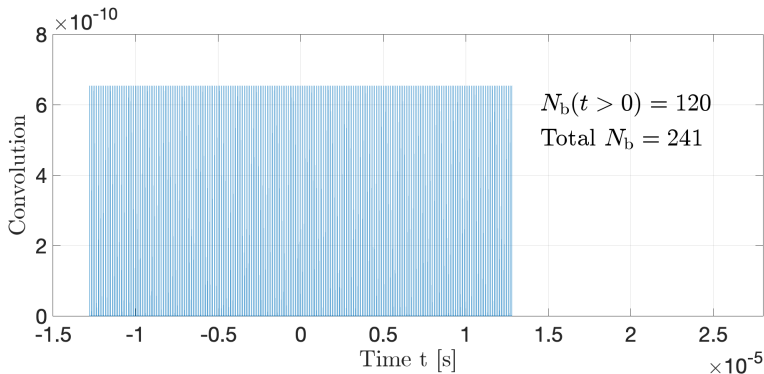
Pulse shape described by

$$f(t) = \frac{Q}{\sqrt{2\pi}\sigma_t} \exp\left(-\frac{t^2}{2\sigma_t^2}\right) \quad (7)$$

# Gaussian convoluted with (finite) series of delta functions

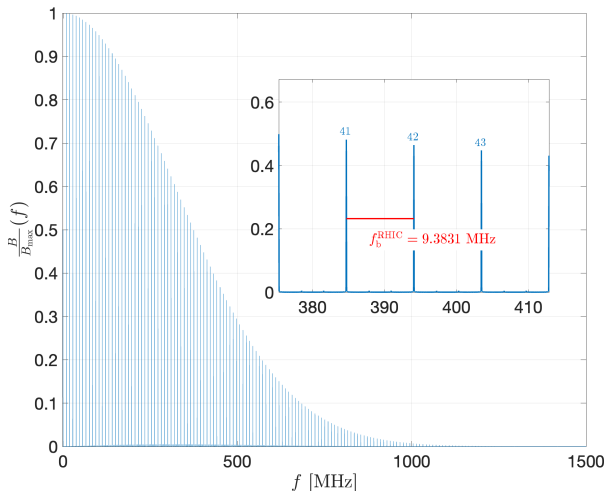
Total beam current as function of time  $t$  given by

$$I(t) = \int_{-\infty}^{\infty} f(t - \xi) \sum_{k=-\infty}^{\infty} \delta\left(\xi - k \frac{\tau_{\text{rev}}}{N_b}\right) d\xi \quad (8)$$



# Produced radio-frequency fields from FFT of convolution

- Single-sided amplitude spectrum of FFT
- x-axis converted to frequency



# Transition frequencies between hyperfine states of H

Based on Zeeman splitting (slide 14) using Eq. (6)

- Determine transition frequencies  $f_{ij}$  between hyperfine states  $|i\rangle$  and  $|j\rangle$ .
- Classification refers to change of quantum numbers (see Ramsey [4]):
  - $B_0$  is static field,  $B_1$  is RF field that exerts torque on magnetic moment  $\mu$ :
  - $\pi$  ( $B_1 \perp B_0$ ) transitions *within one*  $F$  multiplet:

$$\Delta F = 0, \quad \Delta m_F = \pm 1. \quad (9)$$

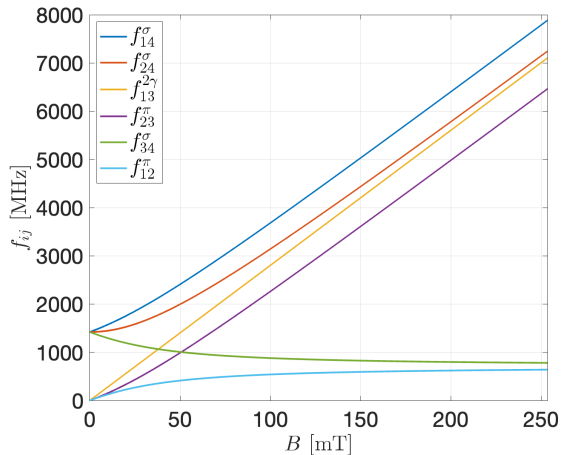
- $\sigma$  ( $B_1 \parallel B_0$ ) transitions *between different*  $F$  multiplets:

$$\Delta F = \pm 1, \quad \Delta m_F = 0, \pm 1. \quad (10)$$

## Possible transitions

- Single photon transitions in H:  $f_{12}^\pi$ ,  $f_{23}^\pi$ ,  $f_{14}^\sigma$ ,  $f_{24}^\sigma$ , and  $f_{34}^\sigma$ .
- Transition  $f_{13}^{2\gamma}$  with  $\Delta m_F = 2$  requires two photons.

# Transition frequencies between hyperfine states of H

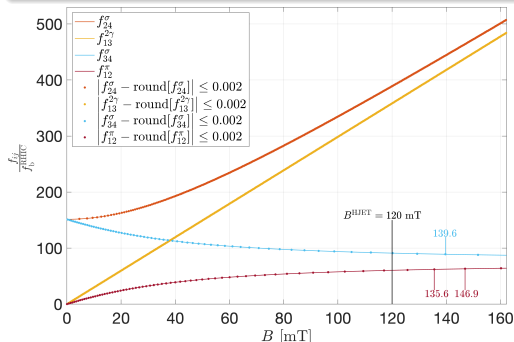


For  $n = 4$  hyperfine states,  $\binom{n}{2} = 6$  transitions possible.

# Hyperfine transitions in H from bunch fields at RHIC

Depolarization occurs when  $f_{ij}$  multiple of bunch frequency  $f_b^{\text{RHIC}}$

- HJET injects states  $|1\rangle + |4\rangle$  ( $p^\uparrow$ ) and  $|2\rangle + |3\rangle$  ( $p^\downarrow$ ).
- What is exact magnitude and orientation of  $\vec{B}^{\text{HJET}}$ ? **Visit issue after run 25**



- $\left| \frac{f_{ij}}{f_b^{\text{RHIC}}} - n \right| \leq 0.002, n \in \mathbb{N}$
- No depolarization from same  $m_l \Rightarrow f_{14}^\sigma, f_{23}^\pi$  omitted

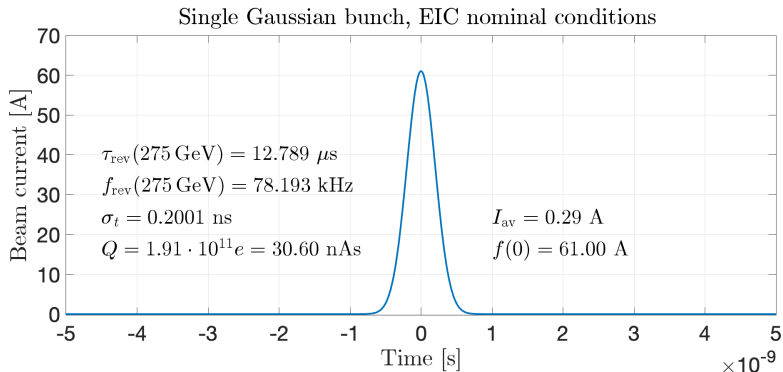
HJET at RHIC operated in safe region around  $B_y = 120$  mT

- At RHIC, transitions with  $\frac{f_{ij}}{f_b^{\text{RHIC}}} \gtrsim 350$  were ignored
- Don't know exactly at which harmonic number, depolarization sets in.



# Single bunch distribution

- (Gaussian) bunch in EIC



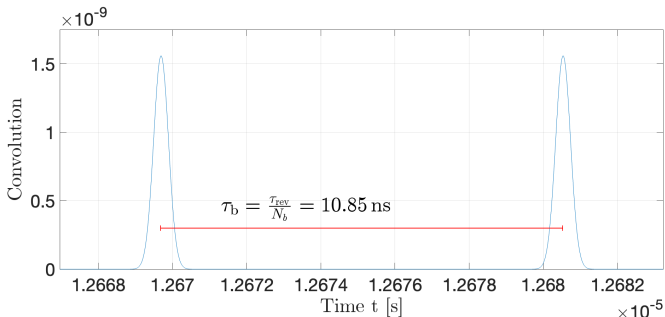
Pulse shape described by

$$f(t) = \frac{Q}{\sqrt{2\pi}\sigma_t} \exp\left(-\frac{t^2}{2\sigma_t^2}\right) \quad (11)$$

# Bunch structure

## EIC situation:

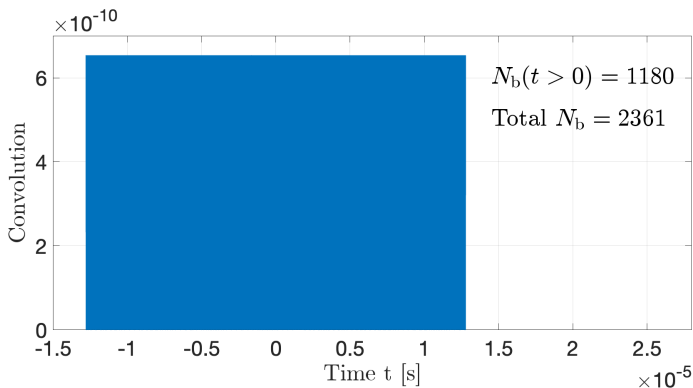
- Time period between two adjacent bunches:  $\tau_b = \frac{\tau_{\text{rev}}}{N_b} = 10.85 \text{ ns}$
- Number of stored bunches  $N_b = 1160$
- Bunch frequency  $f_b = \frac{1}{\tau_b} = 92.2081 \text{ MHz}$



# Gaussian convoluted with (finite) series of delta functions

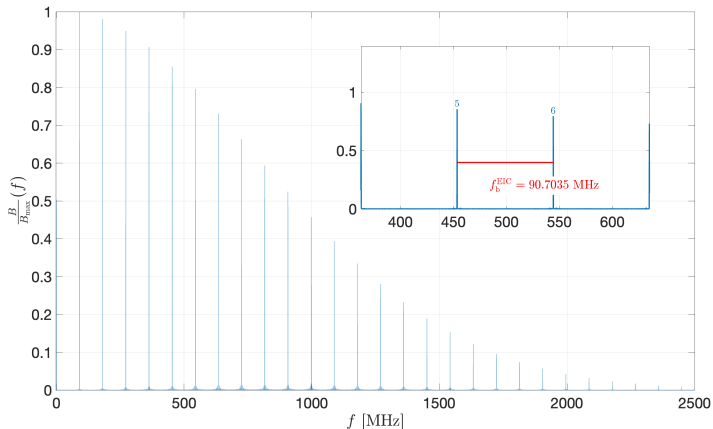
Total beam current as function of time  $t$  given by

$$I(t) = \int_{-\infty}^{\infty} f(t - \xi) \sum_{k=-\infty}^{\infty} \delta\left(\xi - k \frac{\tau_{\text{rev}}}{N_b}\right) d\xi \quad (12)$$



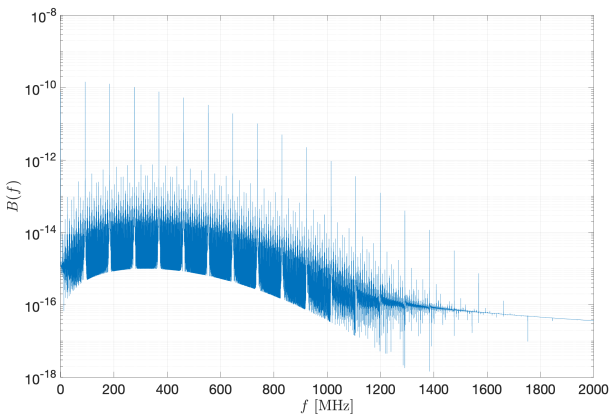
# Produced radio-frequency fields

- Single-sided amplitude spectrum of FFT

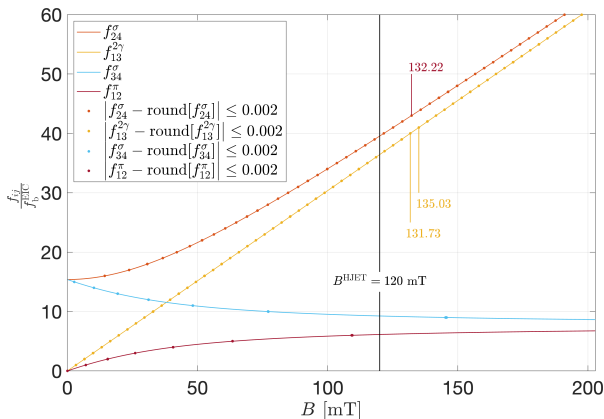


# Amplitudes of radio-frequency fields

- Frequency spacing becomes larger at EIC  $\Rightarrow$  fewer resonances contribute
- RF field amplitudes at EIC  $\approx 10\times$  larger compared to RHIC  
 $\Rightarrow$  increased transition probability due more photons ( $n_\gamma \propto B^2$ ).



# Hyperfine transitions in H from bunch fields at EIC



Depolarization (numerically) occurs when

$$\left| \frac{f_{ij}}{f_b^{\text{EIC}}} - n \right| \leq 0.002, \quad n \in \mathbb{N}$$

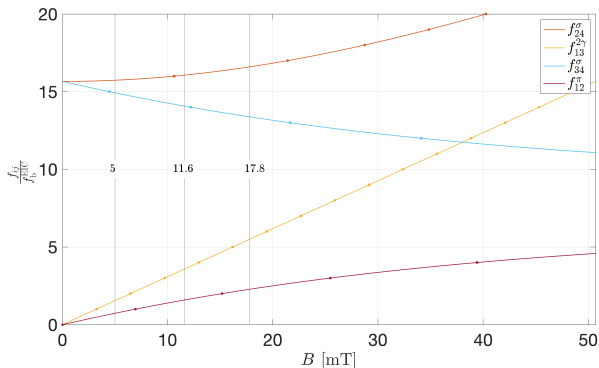
In contrast to RHIC, for  $B < 200 \text{ mT}$

- all transitions below harmonic number  $\approx 60$  contribute at EIC!

# Hyperfine transitions in H from bunch fields at EIC

How about the region of small  $B$ ?

- At RHIC, this region was inaccessible, as spacing of  $f_{13}^{2\gamma} \approx 0.3$  mT.
- At EIC, at  $\approx 5$  mT, spacing of  $f_{13}^{2\gamma} \approx 3.3$  mT.



# Magnetic field from beam charge

## RHIC

### Moving charge of beam induces magnetic field at HJET target

- $\beta$  functions at the HJET in IP12 from G. Robert-Demolaize, 23.07.2024 for RHIC at top energy, determined from fill #34819,

$$\beta_x = 8.243 \text{ m}, \beta_y = 8.326 \text{ m} \quad (13)$$

$$\beta_x = 8.303 \text{ m}, \beta_y = 8.252 \text{ m}$$

- Assume in the following an average  $\bar{\beta}_{\text{jet}} = 8.281$
- Since  $\beta_x \approx \beta_y$ , we deal with a round beam. The normalized RMS emittance taken from the RHIC dashboard during run 24 is:

$$\varepsilon_{\text{rms}}^N = 2.5 \text{ } \mu\text{m} . \quad (14)$$



# Beam parameters for RHIC

- For a Gaussian beam, assume a current density of

$$J = \frac{I(t)}{2\pi\sigma_r^2} \exp\left(-\frac{r^2}{2\sigma_r^2}\right), \quad \text{where} \quad \sigma_r = \sqrt{\frac{\bar{\beta}_{\text{jet}}\epsilon_{\text{rms}}^N}{k \cdot \beta\gamma}} \quad (15)$$

- Due to symmetry of problem, magnetic field  $\vec{B}$  will be tangential to concentric circles around z-axis. Thus,  $\vec{B}$  can be written as

$$\vec{B} = B(r)\vec{e}_\phi \quad (16)$$

- With beam traveling in  $\vec{e}_z$  direction, the integration for a cylindrical Gaussian beam yields flux density

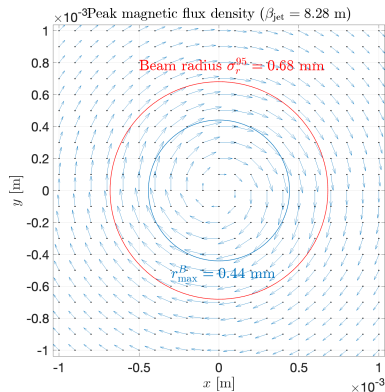
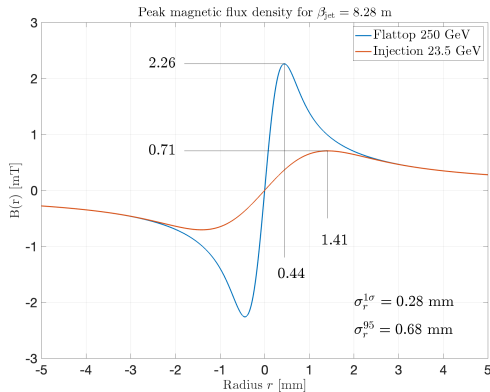
$$\vec{B}(r) = \frac{\mu_0 I(t)}{2\pi r} \left[1 - \exp\left(-\frac{r^2}{2\sigma_r^2}\right)\right] \vec{e}_\phi, \quad \text{with } \vec{e}_\phi = \vec{e}_z \times \vec{e}_r \quad (17)$$

- 

Emittance <sup>2</sup>	Beam width	injection 23.5 GeV	flattop 250 GeV
$\epsilon_{\text{rms}}^N = 2.5 \mu\text{m}$	$\sigma_r^{1\sigma} = \left(\bar{\beta}_{\text{jet}} \cdot \frac{\epsilon_{\text{rms}}^N}{\beta\gamma}\right)^{\frac{1}{2}}$	0.89 mm	0.28 mm
$\epsilon_{95}^N = \epsilon_{\text{rms}}^N \cdot 5.993$	$\sigma_r^{95} = \sigma_r^{1\sigma} \cdot \sqrt{5.993}$	2.18 mm	0.68 mm

<sup>2</sup>Factor 5.993 to convert 1D rms emittance to emittance for 95% of particles in a beam [5].

# Magnetic field from beam charge at RHIC



# Effect of induced magnetic field on jet pol at RHIC

- Systematic variation of magnetic holding field in region struck by beam:
- In center ( $r = 0$ ),  $|\vec{B}(r)| = B_y^{\text{nom}} = 120 \text{ mT}$
- Inside beam, magnetic fields are modified

$$\frac{\int_0^{\sigma_r^{95}} B(r) dr}{\sigma_r^{95}} = 1.73 \text{ mT} \quad (18)$$

- In midplane ( $y = 0$ ), still  $\vec{B} \parallel \vec{e}_y$ .
  - Left hemisphere:  $\vec{B}^L = 121.73 \text{ mT}$ , Right hemisphere:  $\vec{B}^R = 118.27 \text{ mT}$

Relative change of target polarization inside beam is, e.g.,

$$\delta P = \frac{P_{|1\rangle+|4\rangle}(\vec{B}^L) - P_{|1\rangle+|4\rangle}(\vec{B}^R)}{P_{|1\rangle+|4\rangle}(B_y^{\text{nom}})} \leq 0.21\% \quad (19)$$

- In vertical plane ( $x = 0$ ),  $\vec{B} \nparallel \vec{e}_y$ .

## Conclusion for RHIC

- No depolarization due to variation of  $B$  inside beam (slide 20)
- Effect small/tolerable in terms of syst. contribution to jet polarization

# Beam parameters

## EIC

### EIC beam parameters taken from Conceptual Design Report [6]

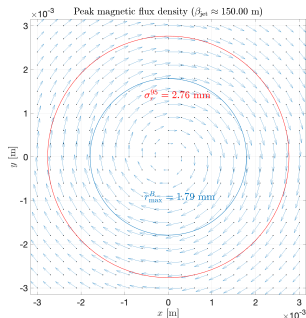
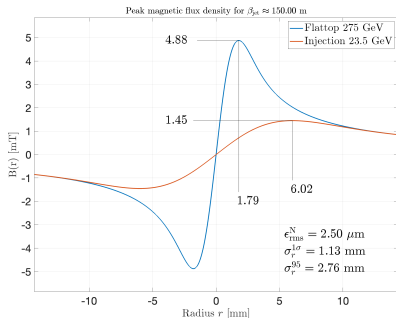
- 275 GeV
- $\beta$ -functions:
  - $\beta_x = 230.323$  m
  - $\beta_y = 69.935$  m
  - $\rightarrow$  assumed in the following:  $\bar{\beta} \approx 150$  m for future location of HJET at IP4 (from H. Lovelace, 31.07.2024).
- Like before,  $\epsilon_{95}^N = \epsilon_{\text{rms}}^N \cdot 5.993$
- Two situations for IP4:

Beam	$\epsilon_{\text{rms}}^N$ [ $\mu\text{m}$ ]	$\sigma_r^{1\sigma}$ [mm]	$\sigma_r^{95}$ [mm]
uncooled	2.5	1.13	2.76
cooled	0.47	0.49	1.20

# Magnetic field from beam charge

EIC

## Uncooled beam



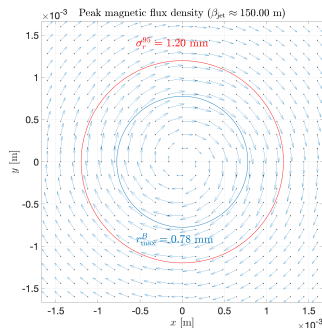
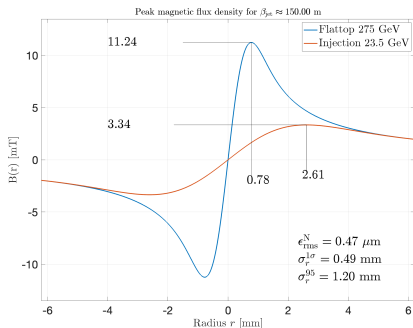
## HJET beam size

- On flattop, transverse dimensions of uncooled proton beam at IP4 comparable to HJET beam diameter (6 mm FWHM  $\rightarrow \sigma^{\text{HJET}} \approx 2.55 \text{ mm}$ ).

# Magnetic field from beam charge

EIC

## Cooled beam



# Effect on magnetic field at jet target and its polarization

## EIC

### Implications for EIC

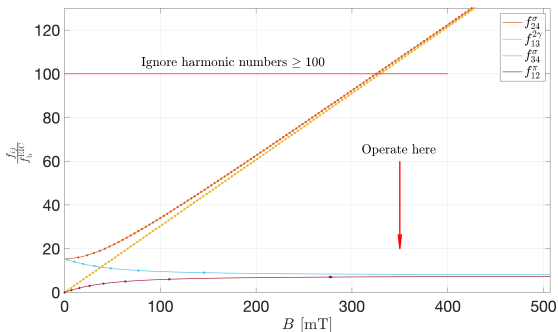
1. Induced B field from beam charge:
  - uncooled beam:  $B(r) \leq 4.88 \text{ mT}$
  - cooled beam:  $B(r) \leq 11.74 \text{ mT}$

→ kills idea to apply weak holding field (20 mT) at target (slide 27)
2. Variation of polarization inside target area at 120 mT [Eq. (19)]:
  - uncooled beam:  $\delta P = 0.45\%$
  - cooled beam:  $\delta P = 1.05\%$
3. Variation of polarization inside target area at 300 mT [Eq. (19)]:
  - uncooled beam:  $\delta P = 0.1\%$
  - cooled beam:  $\delta P = 0.1\%$
4. **Due to fields induced by beam charge (item 1), beam-induced depolarizing resonances appear in HJET target (slide 26)**

# Mitigation of beam-induced magnetic field effect at EIC

## Possible solutions

1. At RHIC, B-field was moved to  $\approx 120$  mT and  $\frac{f_{ij}}{f_b^{\text{RHIC}}} \geq 350$  ignored (slide 20)
2. **Strategy for EIC:  $\Rightarrow$  push harmonics to  $\geq 100 \Rightarrow$  holding field  $\geq 350$  mT**



Where exactly is cutoff located for  $f_{24}^\sigma$  and  $f_{13}^{2\gamma}$ ?

- What is known from RHIC or could still be learned about at which  $B$  field, harmonics become harmless?



# Concept for magnetic guide field for HJET at EIC

But first ...

## Spin-dependent $pp$ elastic cross section (spin 1/2 + spin 1/2)

With polarized beam  $\vec{P}$  and polarized target  $\vec{Q}$ , all components of  $\vec{P}$  can be determined from spin-dependent cross section, as shown in Table below [7, 8]:

$$\begin{aligned} \sigma/\sigma_0 = & 1 + A_y [(P_y + Q_y) \cos \phi - (P_x + Q_x) \sin \phi] \\ & + A_{xx} [P_x Q_x \cos^2 \phi + P_y Q_y \sin^2 \phi + (P_x Q_y + P_y Q_x) \sin \phi \cos \phi] \\ & + A_{yy} [P_x Q_x \sin^2 \phi + P_y Q_y \cos^2 \phi - (P_x Q_y + P_y Q_x) \sin \phi \cos \phi] \\ & + A_{xz} [(P_x Q_z + P_z Q_x) \cos \phi + (P_y Q_z + P_z Q_y) \sin \phi] + A_{zz} P_z Q_z \end{aligned}$$

- Full angular distributions of all  $A_{ik}$ 's were determined.
- Single input:  $A_y = 0.2122 \pm 0.0017$  at  $\theta_{\text{lab}} = 8.64^\circ \pm 0.07^\circ$  [9], known from  $A_y = 1$  point in  $p + {}^{12}\text{C}$  elastic scattering [10].

## Most importantly in context

- determination of beam  $\vec{P} = (P_x, P_y, P_z)$  and target  $\vec{Q} = (Q_x, Q_y, Q_z)$ , as well as non-flipping components possible (slide 72)

# Spin-dependent $pp$ elastic cross section

The above is relevant for two reasons

1. The spin-dependence of  $\vec{p}\vec{p}$  elastic scattering allows to reconstruct angular distributions of all (in that case five) polarization observables.
2. With suitable magnetic guide field, target polarization  $\vec{Q}$  can be oriented along any direction, for instance along  $x$ , so that  $\vec{Q} = Q \cdot \vec{e}_x = \vec{Q}_x$ 
  - Absolute value of target polarization  $Q$  determined by BRP

**Two things needed to port HJET from RHIC to EIC with  $\frac{\Delta P}{P} \leq 1\%$**

1. Substantially stronger holding field of  $|\vec{B}| \approx 300$  to 350 mT than at RHIC
2. Detector capable to pick up azimuthal asymmetries  $\propto \sin \phi$  and  $\propto \sin 2\phi$  (slide 71)
  - foresee proper detector symmetry to provide  $\vec{d}\vec{d}$  beam absolute polarimetry, i.e., beyond  $\propto \sin 2\phi$ .

# Holding field system for $|\vec{B}| \approx 0.3 \text{ T}$ with $\vec{B} \parallel \vec{e}_{x,y,z}$

Work in part together with Helmut Soltner (FZJ, Germany)

## Motivation:

- Reconcile strong magnetic holding field with open detector geometry to determine, e.g., all spin components of beam polarization  $\vec{P} = (P_x, P_y, P_z)$
- Exploit magnetic moments  $\vec{m}$  of homogeneously magnetized spheres [11–13]
- Invert  $\vec{m}$  in vacuum to reverse  $\vec{B}(O)$
- Reorient  $\vec{m}$ 's to generate  $\vec{B}(O) \parallel \vec{e}_{x,y,z}$

## Consider two sets of frames

- Beam meets atoms at  $(O)$ 
  - Set 1:  $100 \text{ mm}_x \times 100 \text{ mm}_y \times 40 \text{ mm}_z$
  - Set 2:  $100 \text{ mm}_x \times 100 \text{ mm}_y \times 110 \text{ mm}_z$
  - 8 magnetized spheres in corners of frames:
  - NeFeB magnets provide remanence of  $B_r = 1.49 - 1.55 \text{ T}$  (type N58)
  - Radius  $r = 30 \text{ mm}$

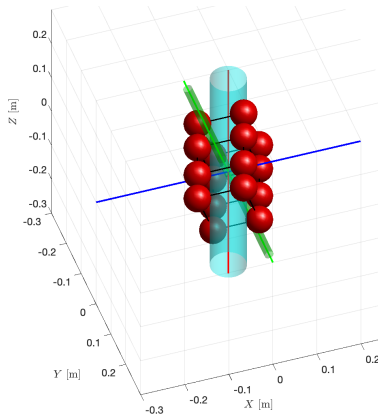
# Holding field system: Calculation

- Flux density vector as fct of  $\vec{m}$  in space

$$\vec{B}(\vec{r}) = \frac{\mu_0}{4\pi} \left[ \frac{3(\vec{m} \cdot \hat{R})\hat{R} - \vec{m}}{|\vec{R}|^3} \right] \quad (20)$$

$$\vec{R} = \vec{r} - \vec{r}_0, \hat{R} = \frac{\vec{R}}{|\vec{R}|}$$

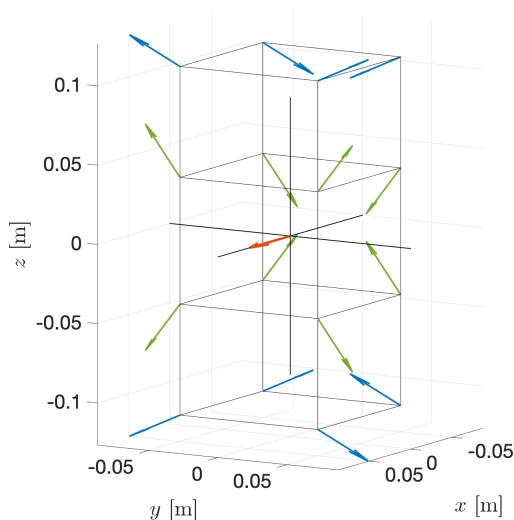
- Optimize orientation of  $\vec{m}$ 's to maximize  $\vec{B}(O)$  along  $\vec{e}_x$ ,  $\vec{e}_y$ , or  $\vec{e}_z$ 
  - maximize dot product  $\vec{m} \cdot \hat{R}$ , set  $m_y = 0$  to obtain, e.g., max.  $B_y$



16 spherical magnetic dipoles

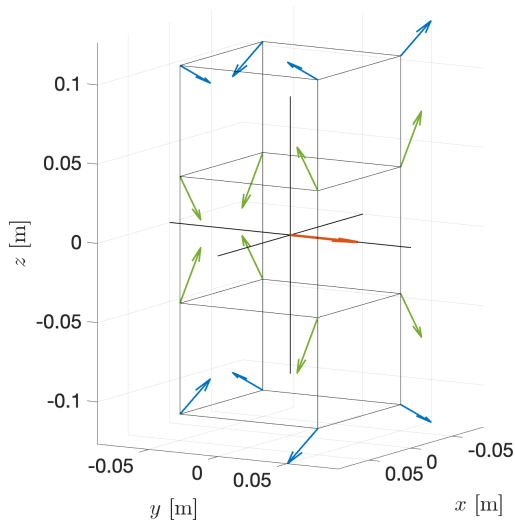
- atomic beam  $\parallel \vec{e}_y$
- ion beam  $\parallel \vec{e}_z$

# Component $B_x(O)$ using two sets of $\vec{m}$ 's



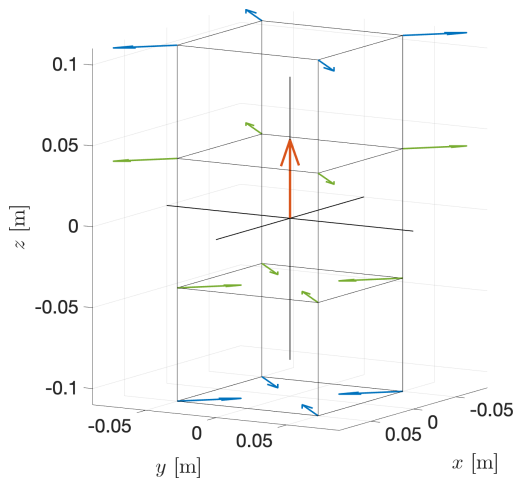
$$B_x: \begin{pmatrix} 0.3224 \\ 0 \\ 0 \end{pmatrix} \text{ T}$$

# Component $B_y(O)$ using two sets of $\vec{m}$ 's



$$B_y: \begin{pmatrix} 0 \\ 0.3224 \\ 0 \end{pmatrix} \text{ T},$$

# Component $B_z(O)$ using two sets of $\vec{m}$ 's



$$B_z: \begin{pmatrix} 0 \\ 0 \\ 0.3227 \end{pmatrix} \text{ T}$$

# Technical realization

LDRD C application (I'm told it's approved, but not official yet)

## With properly rotated spheres

- Setup allows for azimuthally symmetric detector setup with acceptance  $\Delta\phi \approx \pm 20^\circ$  at  $\phi = 45, 135, 225, \text{ and } 315^\circ$ 
  - Slides 71 and 72 show azimuthal acceptance could look like
- **Technical challenges:**
  1. Accurate 3D reorientation of magnetized spheres<sup>a</sup> in vacuum [14]
  2. Vacuum compatible coating, like Ni, or stainless steel covers to prevent H and H<sub>2</sub> from deteriorating NeFeB
  3. **First Step: build a lab test setup and verify concept is technically sound**
  4. Forces and torques appear manageable (next slides)

---

<sup>a</sup><https://www.youtube.com/watch?v=hhDdfiRCQS4>



# Force and torque between two dipoles $\vec{m}_1$ and $\vec{m}_2$ I

## Potential energy of magnetic dipole

$$U = -\vec{m} \cdot \vec{B}$$

$$\vec{F} = -\vec{\nabla} U \quad \rightarrow \quad F_{12} = \vec{\nabla} (\vec{m}_2 \cdot \vec{B}_1)$$
(21)

- $\vec{B}_1$  is flux density produced by  $\vec{m}_1$  at location of  $\vec{m}_2$ .

## Force:

$$\vec{F}_{12}(\vec{r}_{12}, \vec{m}_1, \vec{m}_2) = \frac{3\mu_0}{4\pi r_{12}^4} \left[ \vec{m}_2 (\vec{m}_1 \cdot \vec{e}_{12}) + \vec{m}_1 (\vec{m}_2 \cdot \vec{e}_{12}) + \vec{e}_{12} (\vec{m}_1 \cdot \vec{m}_2) - 5\vec{e}_{12} (\vec{m}_1 \cdot \vec{e}_{12}) (\vec{m}_2 \cdot \vec{e}_{12}) \right]$$
(22)

- $\vec{r}_{12}$  is vector between  $\vec{m}_1$  and  $\vec{m}_2$ ,  $\vec{e}_{12} = \frac{\vec{r}_{12}}{|\vec{r}_{12}|}$ .

## Torque

$$\vec{\tau} = \vec{m}_2 \times \vec{B}_1$$
(23)

# Force and torque between two dipoles $\vec{m}_1$ and $\vec{m}_2$ II

Examples:  $\vec{m}_1 \perp \vec{m}_2$

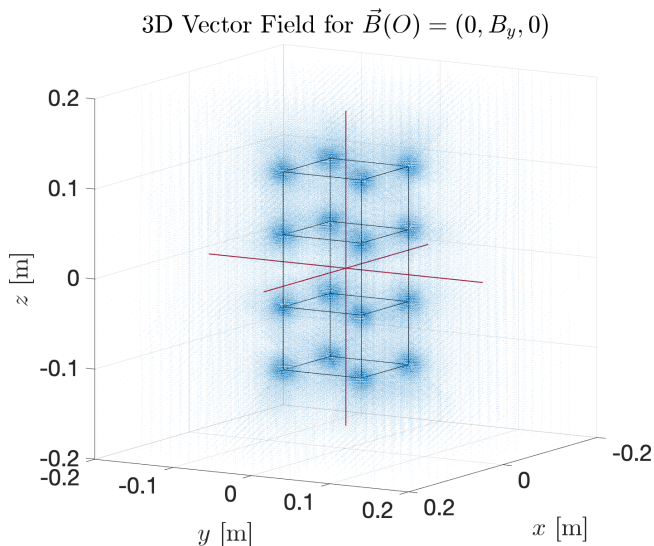
1. Spheres touch:

$$r_{12} = 0.06 \text{ m} \quad \vec{F}_{12} = -417 \text{ N} \quad \tau_{12} = 8.3 \text{ Nm} \quad (24)$$

2. System assembled:

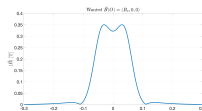
$$r_{12} \geq 0.07 \text{ m} \quad \vec{F}_{12} \leq -225 \text{ N} \quad \tau_{12} = 5.2 \text{ Nm} \quad (25)$$

# Flux density of system in 3D

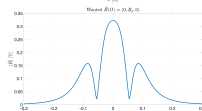


# No zero crossings along axes

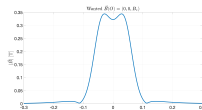
$$\vec{B}(O) \parallel \vec{e}_x$$



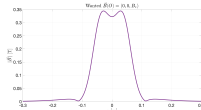
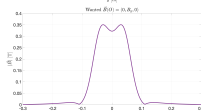
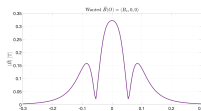
$$\vec{B}(O) \parallel \vec{e}_y$$



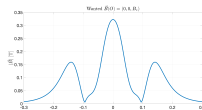
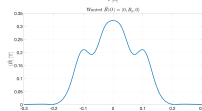
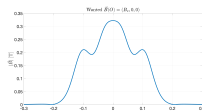
$$\vec{B}(O) \parallel \vec{e}_z$$



x



y



z

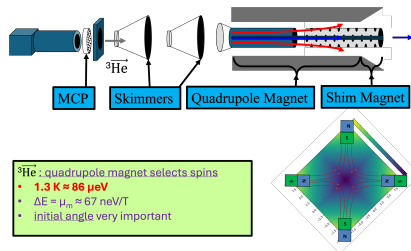
- No zero crossing of magnetic field along vertical jet (y) axis
- $B_y^{\min} \approx 1.9$  mT sufficient to avoid Majorana depolarization
- Field integrals along beam (z) axis

$\vec{B}(O)$	$\parallel \vec{e}_x$	$\parallel \vec{e}_y$	$\parallel \vec{e}_z$
$\int  \vec{B}  dz$	0.0667 Tm	0.0667 Tm	0.0546 Tm

# Polarized $^3\text{He}$ Atomic Beam Source

## Original MIT development for nEDM exp't at Oakridge

- Prajwal T. MohanMurthy, J. Kelsey, J. Dodge, R. Redwine, R. Milner, P. Binns, B. O'Rourke
- nEDM experiment at ORNL discontinued



## High atomic flux

- $\geq 1 \times 10^{14} \text{ atoms/s} \rightarrow d_t \geq 1 \times 10^{13} \text{ atoms/cm}^2$
- Ideal device for absolute  $^3\vec{\text{He}}^{++}$  beam polarimetry at EIC

# Absolute polarimetry of $\vec{d}$ beams

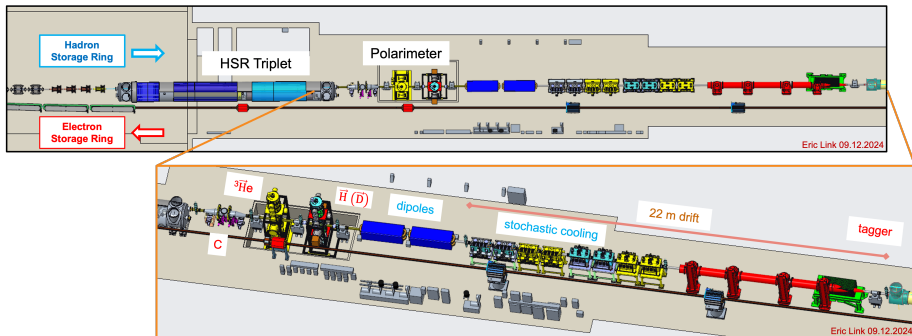
## Polarized atomic deuterium jet

- Atomic beam sources efficiently produce beams of deuterium atoms
- Ideal would be the use of dual-function RF transition units for  $\vec{H}$  and  $\vec{D}$  atoms
- With vector and tensor polarization accurately determined by BRP, absolute beam polarimetry based on  $\vec{d}\vec{d}$  elastic scattering becomes possible
  - + reconstruction of 3D polarization vector, including tensor components.

# EIC hadron polarimetry at IP4

## Carbon, polarized H and $^3\text{He}$ gas targets

- Important to set up all polarimeters in one place without much drift, magnetic elements, etc, to minimize spin rotation between them



# Will carbon fiber targets survive at EIC?

## Target heating calculated according to Peter Thieberger

- With proper beam sizes, there is not much difference between RHIC and EIC.
- RF heating of the target supports not included, will be more severe at EIC due to shorter bunches.
- RF design of target holders needs to be optimized.





# Carbon target temperatures from Thieberger's estimate

## RHIC typical conditions

- 250 GeV
- 111 bunches
- $16 \times 10^{10}$  protons per bunch
- $\sigma_r^{95} = 0.68$  mm (slide 29)

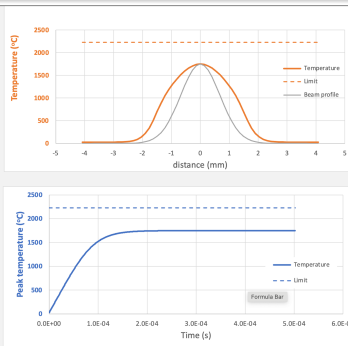
TARGET	GRAPHITE	TUNGSTEN	CARBON
Density (g/cc)	2.26	19.3	2.26
LET (MeV cm <sup>2</sup> /g)	1.76E-03	1.12E-03	6.33E-04
Thermal conductivity [W/(K * m)]	390	173	390
Emissivity	0.8	0.35	0.8
Specific heat (J/(gm K))	0.72	0.134	0.72
Thickness (nm)	50	100	50
Sublimation or melting limit (°C)	2227	3422	2227

PROTON BEAM	RHIC 2017	EIC	XX bunch
Beam rms width (mm)	0.68	1.2	
# of protons per bunch	1.60E+11	6.90E+10	
# of bunches	111	1160	

Thermal conductivity multiplier	1
Simulation time step (ns)	500



# Carbon target temperatures from Thieberger's estimate

## EIC for highest luminosity

- 275 GeV
- 1160 bunches
- $6.9 \times 10^{10}$  protons per bunch
- $\sigma_r^{95} = 1.2$  mm **cooled beam**

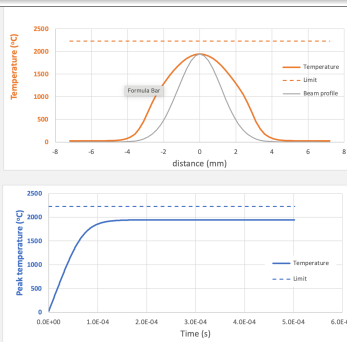
TARGET	GRAPHITE	TUNGSTEN	CARBON
Density (g/cc)	2.26	19.3	2.26
LET (MeV cm <sup>2</sup> /g)	1.74E-03	1.12E-03	6.33E-04
Thermal conductivity (W/(K * m))	390	173	390
Emissivity	0.8	0.35	0.8
Specific heat (J/(kg K))	0.72	0.134	0.72
Thickness (nm)	50	100	50
Sublimation or melting limit (°C)	2227	3422	2227

PROTON BEAM	RHIC 2017	EIC	XX bunch
Beam rms width (mm)	0.68	1.2	
# of protons per bunch	1.60E+11	6.90E+10	
# of bunches	111	1160	

Thermal conductivity multiplier	1
Simulation time step (ns)	500



# Carbon target temperatures from Thieberger's estimate

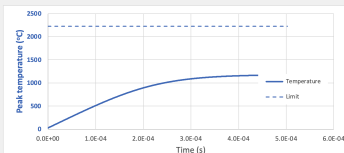
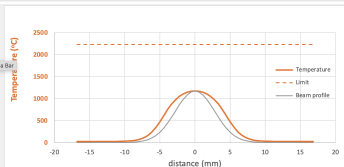
## EIC for highest luminosity

- 275 GeV
- 1160 bunches
- $6.9 \times 10^{10}$  protons per bunch
- $\sigma_r^{95} = 2.8$  mm **uncooled beam** (slide 32)

TARGET	GRAPHITE	TUNGSTEN	CARBON
Density (g/cc)	2.26	19.3	2.26
LET (MeV cm <sup>2</sup> /g)	1.76E-03	1.12E-03	6.33E-04
Thermal conductivity [W/(K * m)]	390	173	390
Emissivity	0.8	0.35	0.8
Specific heat (J/(gm K))	0.72	0.134	0.72
Thickness (mm)	50	100	50
Sublimation or melting limit (°C)	2227	3422	2227

PROTON BEAM	RHIC 2017	EIC	XX bunch
Beam rms width (mm)	0.68	2.8	
# of protons per bunch	1.60E+11	6.90E+10	
# of bunches	111	1160	

Thermal conductivity multiplier	1
Simulation time step (ns)	500



# Direct measurement of temperature of carbon targets

Work with Vera Shmakova, Prashanth Shanmuganathan, Oleg Eyser, Haixin Huang, Dannie Steskie, Thomas Tsang, and George Mahler

- Carbon fiber targets of RHIC polarimeters do not reach carbon sublimation temperature of  $T_{\text{sub}} = 3915 \text{ K}$ : **targets survive proton bombardment**.
  - Observation aligns with energy loss calculations by Peter Thieberger (BNL) using appropriate beam sizes at the interaction point.
- Direct temperature measurement of carbon targets remains crucial goal
  - Black-body radiation [15] as a method to determine temperature by analyzing the emitted light spectrum.
- **APEX measurement approved for run 25**
  - more details on this investigations on slides slides 73 – 77

# Conclusion and Outlook I

## 1. Bunch-induced depolarization in H target

- RHIC: harmonic numbers  $> 350$  were ignored
- EIC: All depolarizing transitions appear at harmonic numbers  $< 50$

## 2. Beam-induced magnetic fields perturb target polarization

- RHIC: Magnetic field involved:  $B(r) \leq 2.3 \text{ mT}$
- EIC: uncooled  $B(r) < 4.9 \text{ mT}$
- EIC: cooled  $B(r) < 11.7 \text{ mT}$

## 3. Solution for 1. and 2.: Holding field of $|\vec{B}| \geq 300 \text{ mT}$

- Concept using permanent magnets (NdFeB) appears feasible
  - FY2025 LDRD C approved to demonstrate feasibility
- Allows for orientation of holding field  $\vec{B}$  in any direction (along x, y, or z)
- System will allow to provide holding field  $\vec{B} = 0$
- No zero crossings along ABS axis,  $|\vec{B}(0, y, 0)| \gtrsim 1.9 \text{ mT}$
- May need compensation scheme to make  $\int B_{x,y,z} d\ell = 0$  along beam (z) axis
  - What's the spin rotation angle along the beam (z) axis?
  - Tolerable? Does one need compensation beyond  $\int B d\ell = 0$ ?

## 4. Early 2026: HJET set up in high bay of 510

# Conclusion and Outlook II

- Refurbish and upgrade system
- Upgrade slow control
- Implement QMA in setup to allow for determination of  $H_1$  and  $H_2$  contribution in the target

## 5. C targets

- Heating at highest EIC luminosity will be about same as at RHIC, due to much larger  $\beta$  function at IP4 compared to IP12
- C target holder need to be redesigned to minimize increased RF heating at EIC
- Suggest to upgrade pC chamber with vacuum transfer system to avoid venting the chamber during target installation
- Direct C target temperature measurement underway to further mitigate risks

## 6. $^3\vec{\text{He}}$ atomic beam source under development by MIT

- ideally suited for EIC
- Polarimetry section in IP4 looks good

## 7. $\vec{\text{D}}$ and $^3\vec{\text{He}}$ atomic targets at EIC

- Study bunch-induced depolarization
- Study beam-induced  $\vec{B}$  field effects on target polarizations

# Conclusion and Outlook III

## Other things that need to be looked into

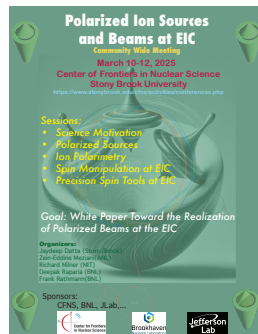
1. Zero-crossings along the vertical axis of present HJET
  - Revisit magnetic field calculations of HJET holding field → in progress.
  - Measure holding field in target region and estimate hysteresis effects
2. Polarization measurements at HJET using all transition units in ABS and BRP after run 25.
3. **Top Priority:** Regain ability to simulate/design polarized atomic beams
  - Critical competence, disappeared from academia in both the US and Europe, **foundational step, absolutely essential**, underpins all future progress.
  - Recuperated tracking code used originally for HJET design from Michelle Stancari/Paolo Lenisa → will be time consuming to make it work
  - **FY2025 LDRD B application pending**
  - A **postdoc of 2 years** will be sufficient to revitalize the critical atomic beam tracking instruments and restore the necessary simulation capabilities.

# Back to my initial observation I

- Key issues include funding, talent recruitment, and securing long-term commitment of new partner institutions
- Future of spin physics with  $\vec{d}$ ,  ${}^3\overline{\text{He}}^{++}$ , or  ${}^{6,7}\overline{\text{Li}}$  beams will no longer even be an option if we wait a few more years to get our act together
- Organize workshops and attract groups from national and international scientific community to work on polarization technology

## Polarized Ion Sources and Beams at EIC

- **Organizers:** J. Datta, Z.-E. Meziani, R. Milner, D. Raparia, and FR
- **Date:** March 10 – 12, 2025
- **Location:** Stony Brook
- **Website:** <https://indico.cfnssbu.physics.sunysb.edu/event/343/>





# References I

- [1] W. Haeberli, "H-jet measures beam polarization at RHIC," CERN Cour. **45N8**, 15 (2005).
- [2] M. Diermaier, C. B. Jepsen, B. Kolbinger, C. Malbrunot, O. Massiczek, C. Sauerzopf, M. C. Simon, J. Zmeskal, and E. Widmann, "In-beam measurement of the hydrogen hyperfine splitting and prospects for antihydrogen spectroscopy," *Nature Commun.* **8**, 5749 (2017), 1610.06392.
- [3] A. Airapetian, N. Akopov, Z. Akopov, M. Amarian, A. Andrus, E. Aschenauer, W. Augustyniak, R. Avakian, A. Avetissian, E. Avetissian, et al., "The hermes polarized hydrogen and deuterium gas target in the hera electron storage ring," *Nuclear Instruments and Methods in Physics Research Section A: Accelerators, Spectrometers, Detectors and Associated Equipment* **540**, 68 (2005), ISSN 0168-9002, URL <https://www.sciencedirect.com/science/article/pii/S0168900204024167>.
- [4] N. Ramsey, *Molecular Beams* (Oxford University Press, 1956).
- [5] S. Lee, *Accelerator Physics* (World Scientific Publishing Company, 2011), ISBN 9789814405287.
- [6] F. Willeke and J. Beebe-Wang, "Electron ion collider conceptual design report 2021," (????), URL <https://www.osti.gov/biblio/1765663>.
- [7] F. Rathmann et al., "Complete angular distribution measurements of pp spin correlation parameters  $A_{xx}$ ,  $A_{yy}$ , and  $A_{xz}$  and analyzing power  $A_y$  at 197.4 MeV," *Phys. Rev. C* **58**, 658 (1998).
- [8] B. von Przewoski et al., "Proton proton analyzing power and spin correlation measurements between 250-MeV and 450-MeV at  $7^\circ \leq \theta(c.m.) \leq 90^\circ$  with an internal target in a storage ring," *Phys. Rev. C* **58**, 1897 (1998).
- [9] B. von Przewoski, H. O. Meyer, P. V. Pancella, S. F. Pate, R. E. Pollock, T. Rinckel, F. Sperisen, J. Sowinski, W. Haeberli, W. K. Pitts, et al., "Absolute measurement of the p+p analyzing power at 183 mev," *Phys. Rev. C* **44**, 44 (1991), URL <https://link.aps.org/doi/10.1103/PhysRevC.44.44>.
- [10] G. Plattner and A. Bacher, "Absolute calibration of spin- $\frac{1}{2}$  polarization," *Physics Letters B* **36**, 211 (1971), ISSN 0370-2693, URL <https://www.sciencedirect.com/science/article/pii/0370269371900712>.

# References II

- [11] P. Blümner and H. Soltner, "Practical Concepts for Design, Construction and Application of Halbach Magnets in Magnetic Resonance," *Applied Magnetic Resonance* **54**, 1701 (2023), ISSN 1613-7507, URL <https://doi.org/10.1007/s00723-023-01602-2>.
- [12] H. Soltner and P. Blümner, "Dipolar halbach magnet stacks made from identically shaped permanent magnets for magnetic resonance," *Concepts in Magnetic Resonance Part A* **36A**, 211 (2010), <https://onlinelibrary.wiley.com/doi/pdf/10.1002/cmr.a.20165>, URL <https://onlinelibrary.wiley.com/doi/abs/10.1002/cmr.a.20165>.
- [13] H. Raich and P. Blümner, "Design and construction of a dipolar halbach array with a homogeneous field from identical bar magnets: Nmr mandhalas," *Concepts in Magnetic Resonance Part B: Magnetic Resonance Engineering* **23B**, 16 (2004), <https://onlinelibrary.wiley.com/doi/pdf/10.1002/cmr.b.20018>, URL <https://onlinelibrary.wiley.com/doi/abs/10.1002/cmr.b.20018>.
- [14] K. Abe, K. Tadakuma, and R. Tadakuma, "Abenics: Active ball joint mechanism with three-dof based on spherical gear meshings," *IEEE Transactions on Robotics* **37**, 1806 (2021).
- [15] M. Planck, *The Theory of Heat Radiation* (P. Blakiston's Son & Co., 1914).
- [16] N. Akchurin, J. Langland, Y. Onel, B. E. Bonner, M. D. Corcoran, J. Cranshaw, F. Nessi-Tedaldi, M. Nessi, C. Nguyen, J. B. Roberts, et al., "Analyzing power measurement of  $pp$  elastic scattering in the coulomb-nuclear interference region with the 200-gev/c polarized-proton beam at fermilab," *Phys. Rev. D* **48**, 3026 (1993), URL <https://link.aps.org/doi/10.1103/PhysRevD.48.3026>.
- [17] I. G. Alekseev, A. Bravar, G. Bunce, S. Dhawan, K. O. Eyser, R. Gill, W. Haeberli, H. Huang, O. Jinnouchi, A. Kponou, et al., "Measurements of single and double spin asymmetry in  $pp$  elastic scattering in the cni region with a polarized atomic hydrogen gas jet target," *Phys. Rev. D* **79**, 094014 (2009), URL <https://link.aps.org/doi/10.1103/PhysRevD.79.094014>.

# References III

- [18] N. H. Buttimore, "A Helium-3 polarimeter using electromagnetic interference," PoS **PSTP2013**, 057 (2013).
- [19] B. v. Przewoski et al., "Analyzing powers and spin correlation coefficients for  $p + d$  elastic scattering at 135 and 200 MeV," Phys. Rev. C **74**, 064003 (2006), URL <http://link.aps.org/doi/10.1103/PhysRevC.74.064003>.
- [20] R. E. Pollock, W. A. Dezarn, M. Dziedzic, J. Duskow, J. G. Hardie, H. O. Meyer, B. v. Przewoski, T. Rinckel, F. Sperisen, W. Haeberli, et al., "Calibration of the polarization of a beam of arbitrary energy in a storage ring," Phys. Rev. E **55**, 7606 (1997), URL <https://link.aps.org/doi/10.1103/PhysRevE.55.7606>.

# Spare slides

# Coulomb-Nuclear interference I

## Need for calibration

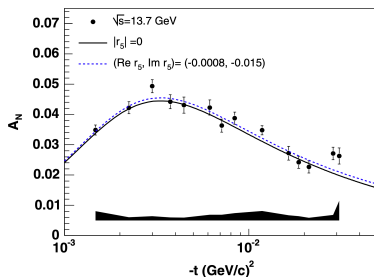
- Asymmetry from CNI region constitutes basis of RHIC high-energy (absolute) polarimeters
  - derived from same EM amplitude that generates anomalous magnetic moment

$$\mu_p = g_p \frac{e\hbar}{2m_p} = g_p \mu_N, \quad g_p \approx 5.585 \quad (26)$$

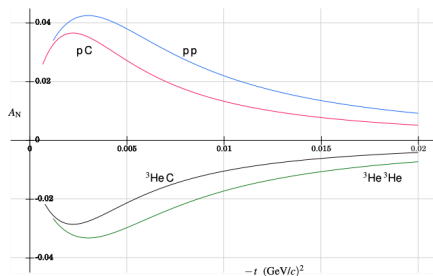
$$g_p - 2 \approx 3.585 \Rightarrow \mu_p^{\text{anomalous}} \approx 1.792 \mu_N$$

- E704 at Fermilab used 200 GeV/c  $\vec{p}$  from hyperon decay to detect asymmetry in scattering from H target [16]. Largest  $A_y \approx 0.04$  with large statistical errors.
- Meanwhile, accurate measurements of  $A_y$  are available from RHIC [17]
- Asymmetry measurements involve normalization uncertainties and calculations of  $A_y$  are subject to uncertainties in amplitudes of strong interaction. **Therefore, accurate calibration of reaction required.**

# Coulomb-Nuclear interference II



Measured  $A_N$  from RHIC in the CNI region at  $\sqrt{s} = 6.8$  GeV ( $E_{\text{lab}} = 23.7$  GeV) [17].



Calculation of  $A_N$  in the CNI region by Nigel Buttimore [18].

# Critical field for hydrogen hyperfine splitting I

## Zeeman region:

- magnetic flux density at which energy separation between different hyperfine levels becomes comparable to Zeeman splitting.
- referred to as *critical magnetic field* or *Breit-Rabi field*  $B_c$
- Breit-Rabi formula (energy levels of hydrogen atom in external magnetic field:

$$E_{F,m_F} = -\frac{E_{\text{hfs}}}{2(2I+1)} + g_J \mu_B m_J B \pm \frac{E_{\text{hfs}}}{2} \sqrt{1 + \frac{2m_F x}{F} + x^2}, \text{ where} \quad (27)$$

- $E_{\text{hfs}}$  is hyperfine splitting energy
- $I$  is nuclear spin (for H,  $I = \frac{1}{2}$ )
- $g_J$  is Landé g-factor
- $\mu_B$  is Bohr magneton
- $m_J$  is magnetic quantum number
- $m_F$  is total angular momentum quantum number
- $x = \frac{g_J \mu_B B}{E_{\text{hfs}}}$
- $F = I + J$  is total angular momentum (for H,  $J = \frac{1}{2}$ )

# Critical field for hydrogen hyperfine splitting II

For H:

- hyperfine splitting energy  $E_{\text{hfs}}$  (1420 MHz):

$$E_{\text{hfs}} \approx 5.874 \times 10^{-6} \text{ eV} \quad (28)$$

- Critical field  $B_c$  is when Zeeman energy  $g_J \mu_B B$  is comparable to  $E_{\text{hfs}}$ . With  $g_J \mu_B B_c \approx E_{\text{hfs}}$ , we get:

$$B_c \approx \frac{E_{\text{hfs}}}{g_J \mu_B} \quad (29)$$

- For H,  $g_J \approx 2$  (approximately for electron), and  $\mu_B \approx 5.788 \times 10^{-5} \text{ eV/T}$ . Thus,

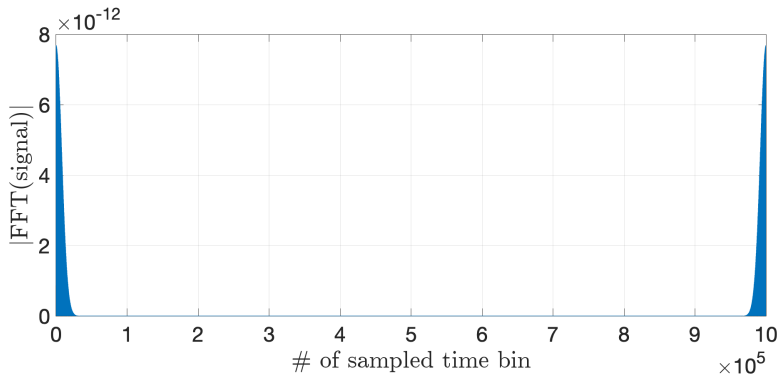
$$B_c \approx \frac{5.874 \times 10^{-6} \text{ eV}}{2 \times 5.788 \times 10^{-5} \text{ eV/T}} \approx 50.7 \text{ mT} \quad (30)$$



# Radiofrequency-fields

## FFT of convolution

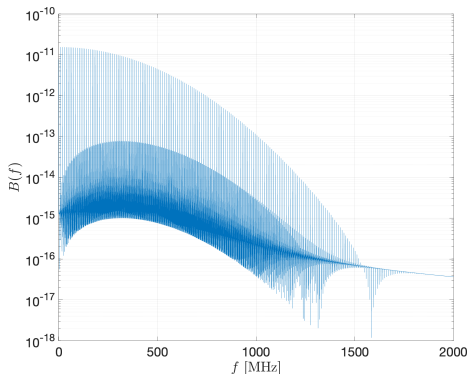
- Two-sided amplitude spectrum of FFT of the convolution



# Amplitudes of magnetic RF fields

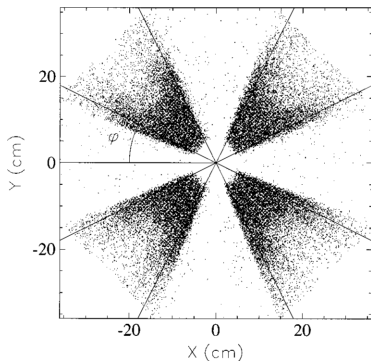
from FFT of convolution

- Same, but logy
- FFT background  $\leq 1\%$ 
  - not at  $f_{\text{rev}}$
  - not from finite set of  $\delta$  fcts
  - $\rightarrow$  probably numerical from FFT



# Detector symmetry required to accomplish the task

**For  $\text{spin } \frac{1}{2} + \text{spin } \frac{1}{2}$  scattering**, suitable geometry below shows pattern of detected azimuthal angles [7].



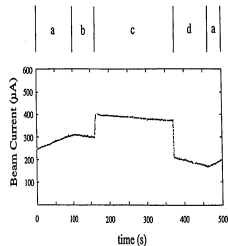
**For  $\text{spin } \frac{1}{2} + \text{spin } 1$  scattering**, a higher segmentation is needed, because besides  $\sin \phi$  and  $\sin 2\phi$ , also terms  $\sin 3\phi, \dots$  contribute to asymmetries [19].

# Polarization of beam $\vec{P}$ and target $\vec{Q}$ [7, 8]

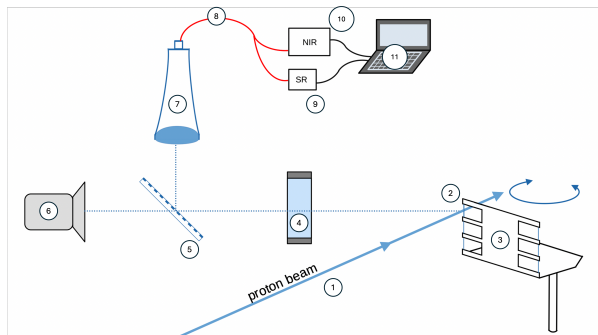
	$\pm x$		$\pm y$		$\pm z$	
	PRE	POST	PRE	POST	PRE	POST
$P_x$	0.0052(47)	0.0089(44)	0.0052(47)	0.0089(44)	0.0052(47)	0.0089(44)
$P_y^a$	<b>0.5801(34)</b>	<b>0.5425(32)</b>	<b>0.5802(34)</b>	<b>0.5417(32)</b>	<b>0.5765(34)</b>	<b>0.5447(32)</b>
$P_z$	-0.0021(47)	0.0003(44)	-0.0021(47)	0.0003(44)	-0.0021(47)	0.0003(44)
$Q_x$	<b>0.7401(59)</b>	<b>0.7394(56)</b>	-0.0039(59)	0.0039(56)	-0.0071(23)	-0.0052(23)
$Q_y$	0.0111(59)	0.0039(56)	<b>0.7400(59)</b>	<b>0.7406(56)</b>	-0.0055(59)	-0.0034(56)
$Q_z$	0.0158(60)	0.0240(60)	-0.0174(61)	-0.0121(61)	<b>0.7401(42)<sup>b</sup></b>	<b>0.7400(40)<sup>b</sup></b>
$S_{P_y}$	-0.0008(18)	-0.0005(17)	-0.0008(18)	0.0005(17)	-0.0008(18)	0.0005(17)
$S_{Q_x}$	0.0017(23)	-0.0007(23)	-0.0040(23)	-0.0031(23)	-0.0043(23)	-0.0024(23)
$S_{Q_z}$	-0.0091(82)	-0.0162(82)	-0.0177(82)	-0.0197(82)	0.0013(82)	-0.0086(82)

- Beam polarization export/calibration to arbitrary energy [20]

- PRE  $\equiv$  b (197.4 MeV)
- Export  $\equiv$  c (399.1 MeV)
- POST  $\equiv$  d (197.4 MeV)



# Experimental setup



① proton beam

② fiber target

③ target holder

④ fused-silica  
viewport

⑤ semi-transparent  
polka-dot mirror

⑥ optical camera

⑦ collimator lens

⑧ fiber splitter (VIS and IR)

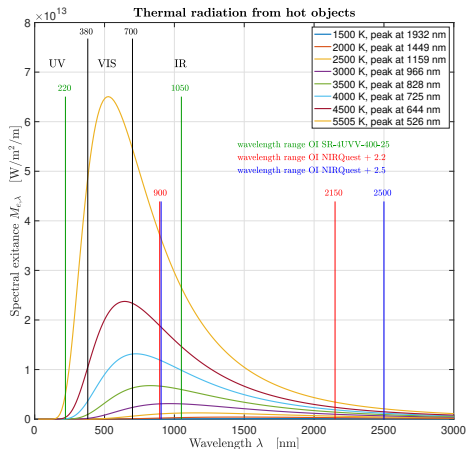
⑨ spectrometer VIS (SR)

⑩ spectrometer IR (NIR)

⑪ spectral analysis  
( $\lambda = 200 - 2200 \text{ nm}$ )

# Black body radiation

Ideally, one would measure:

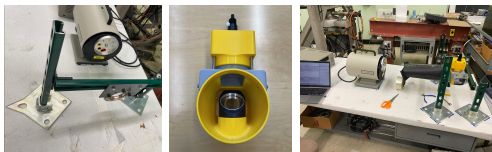


**wavelength-dependent  
attenuation in**

- fused-silica viewport
- collimator lens
- 100 m glass fibers from IP12 to spectrometers

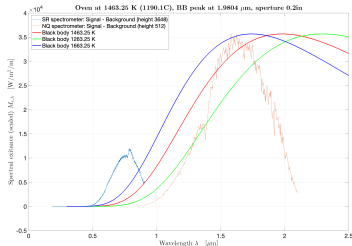
# Lab test measurement using IR light source

## Experimental setup



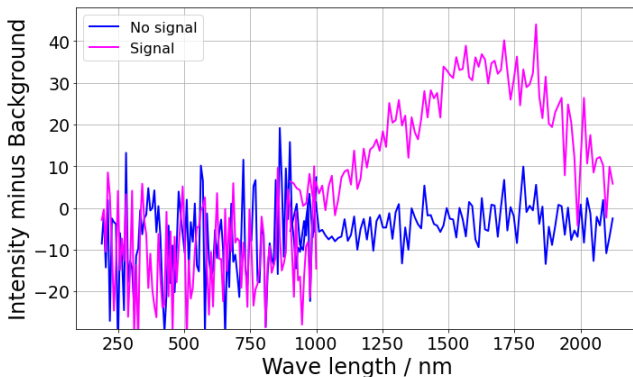
## Black body radiation using oven at 1463 K

- SR spectrometer: 200 to 900 nm
- NIR spectrometer: 900 to 2100 nm
- Light path includes fiber splitter and 100 m glass fibers
- Measured spectrum compared to blackbody radiation spectra at 1463 K, 1263 K, and 1663 K



# Test measurements using C targets at IP4

- In 2024, equipment/components arrived late, thus optimal alignment of light collection system at IP4 was not possible.
- We observe a clear signal, however, the light intensity is low because we don't aim at the brightest spot on the target
- For the same reason, the temperature we observe is only around 1400 K, about half of what we would expect





# APEX proposal

## Goals for run 25

- **Ensure full understanding of energy loss/heating of carbon polarimetry fiber targets by high energy proton beam, in particular for EIC**
- Light collection system was installed and operated already during run 24
  - As CNI chamber was already sealed off/pumped down when all components were available, light collection system could not be properly aligned
- **Improve alignment before ring closes, repeat measurement in run 25**
  1. Our APEX requires dedicated time only in case no proton beam available in run 25. With 100 GeV stored protons, we can run parasitically.
  2. Need 100 GeV protons in blue with max. number of bunches stored
  3. With beam on flattop, a single fill of the machine should be sufficient:
    - Sweep one target back and forth through the beam, then do another one, and so on. No need to wait for target cool down.
    - Will use four targets in blue, two horizontal ones and two vertical ones.
  4. 2h sweeping targets back and forth sufficient to achieve goals
  5. In case something goes wrong with 3. and 4., we need a 2<sup>nd</sup> fill